FACTA UNIVERSITATIS
Series: Architecture and Civil Engineering Vol. 20, Nº 3, 2022, pp. 301-311
https://doi.org/10.2298/FUACE221112022M

Original Scientific Paper

DESIGN OF NAILED TIMBER-CONCRETE COMPOSITE JOINT ACCORDING TO EUROCODE AND FEA

UDC 624.011.1+624.012.4
624.016.04

Miloš Milić, Predrag Petronijević, Todor Vacev, Andrija Zorić, Ivan Nešović

Faculty of Civil Engineering and Architecture, University of Niš, Serbia

Abstract. *During rehabilitation of residential buildings built in the first half of the 20th century, it is necessary to strengthen timber floors so they can fulfill the requirements of strength and serviceability according to contemporary regulations. Floors made of monolithic timber girders can be most easily strengthened by forming a composite structure with a reinforced concrete slab supported on a trapezoidal steel sheeting, with appropriate connections between different materials. In the paper, the procedure of calculation of nails used as shear connectors for composite action of timber and concrete is presented. The procedure is based on equations given in Eurocode 5, and besides that, a calculation applying FEM has been conducted, and a comparison of results is presented.*

Key words: *composite action timber-concrete, nail, rope effect, Eurocode 5, FEM*

1. INTRODUCTION

Composite floors consisted of timber girders and reinforced concrete slab lied on a trapezoidal steel sheeting have broad application in construction. They can be used as for sanation of old timber floors, as well as at newly designed girders. Buildings erected in the first half of the 20th century mostly have floors made of timber girders, and because of their poor state a need for some structural intervention arises. In most cases, the existing structure cannot be kept without some kind of strengthening (Maslak, et al., 2020), because of their unfavorable characteristics regarding vibrations (Kozarić, 2016).

One of the methods of improvement of the characteristics of a timber floor is by composite action with added reinforced concrete slab. As a form, a galvanized steel trapezoidal sheeting TR60/210 with thickness of 0.5-0.6 mm is used in most cases. This

Received November 12, 2022 / Accepted December 6, 2022
Corresponding author: Miloš Milić, University of Niš, Faculty of Civil Engineering and Architecture, Aleksandra Medvedeva 14, 18000 Niš, Serbia
e-mail: milos.milic@gaf.ni.ac.rs

technique increases the mass of the floor structure, which is unfavorable. However, this significantly increases the structural stiffness. Comparing the drawbacks and the benefits of this technique, one may conclude that the final effect is favorable (Milić, et al., 2021). Achieving of the adequate stiffness of the girder could not be possible without appropriate shear connectors, which connect the new reinforced concrete slab with the existing timber girders.

Shear connectors for composite action of timber and concrete can have different forms: nails, bolts, steel bars, steel tubes, carpentry joints, etc. Combinations of different types of dowels can be also used (Stevanović, 2004; Khorsandnia, et al., 2012; Hassanieh, et al., 2016; Stojić and Cvetković, 2001). Contemporary construction practice requires simple and fast installing of shear connectors, with satisfying characteristics regarding their strength and serviceability. Bolts and nails are the most often used types.

In this paper, the strength of the joint of a timber girder and a reinforced concrete slab supported on trapezoidal steel sheeting performed by nails is analytically defined. For the purpose of strength calculation of the joint, the equations according to the Johansen's procedure (Johansen, 1949), adopted in Eurocode (EN 1995-1-1, 2004), are used. Besides that, the joint has been modelled and calculated applying the Finite Element Method (FEM), and the obtained results have been compared with the results of the analytical calculation.

2. SETTING OF THE PROBLEM

In this research, the task was to strengthen timber floor structure presented in **Error! Reference source not found.**. Timber girders with cross section 180/200 mm were set at mutual distance of 800 mm. Timber grade was adopted as C24 (EN 338, 2009). The rehabilitation was performed by concreting the slab over the steel trapezoidal sheeting TR 60/210, that was previously set over the timber girders. The ribs of the trapezoidal sheeting were set perpendicularly to the timber girder direction. After concreting, the thickness of the concrete slab was 110 mm over the troughs, and 50 mm over the ridges of the sheeting. The concrete class was C30/37 (EN 1992-1-1, 2004), and the slab was reinforced by wire-mesh reinforcement Q84.

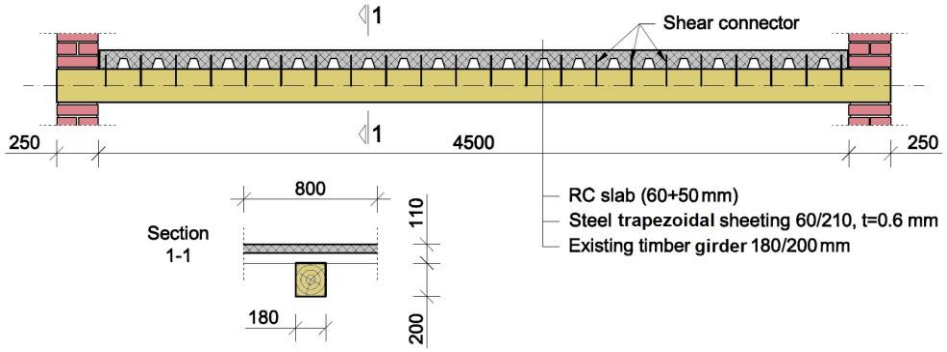

Fig. 1 Disposition of the rehabilitated floor (Milić, et al., 2021)

For joining the timber girder with the reinforced concrete slab, nails E70/200 (Ø7 mm, total length 200 mm) were used. The nails are fabricated of wire with ultimate strength $f_u = 600$ MPa (EN 1995-1-1, 2004). Half of the nail length is embedded in timber, and half in concrete (**Error! Reference source not found.**).

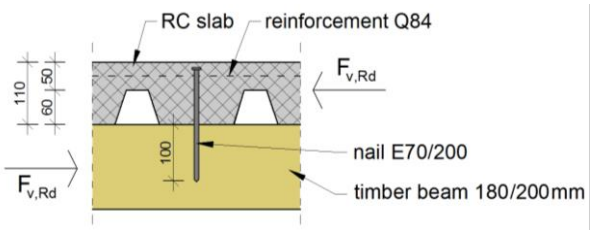

Fig. 2 Detail of the analyzed joint

3. MODES OF FAILURE AND CALCULATION BY EUROCODE 5

The Eurocode 5 standard does not provide an exact procedure for determining the strength of the joint of a timber girder and reinforced concrete slab supported on trapezoidal sheeting performed by nails. However, the equations defined for other joints given in Eurocode may be used, like the joint between a thick steel element and a timber element. In such case, the nail is considered as fixed into the steel element. Applying analogy, this case is used for the research in this paper, whereat instead the steel element, a RC slab is introduced. The stiffness ratio between an RC slab and a timber element is lower than the ratio between steel and timber, but still sufficiently high to justify the analogy used.

Considering the previous, one may say that the RC slab in this joint is absolutely stiff, and therefore it is not a subject of calculation. Taking into account the mentioned analogy and the failure modes for this type of joint given by Eurocode, the following types of failure modes are proposed (**Error! Reference source not found.**).

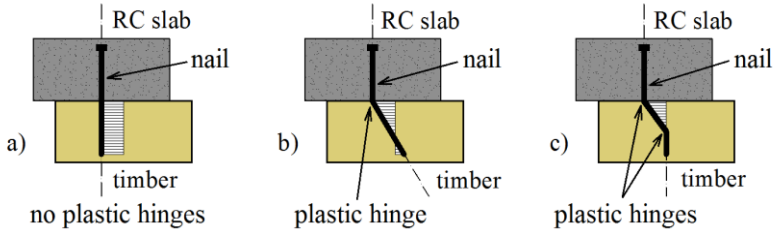

Fig. 3 Possible failure modes of the analyzed joint

The first failure mode of the joint (**Error! Reference source not found.**a) implies that an exceedance of the embedment stress in timber occurs, without forming a plastic hinge in the nail. Such failure mode is unfavorable, because the failure occurs abruptly (brittle failure). In the second failure mode, a plastic hinge occurs in the nail at the slipping plane, and the part of the nail in the timber volume acts as a rigid body (**Error! Reference source not found.**b). In the third failure mode, two plastic hinges arise. Exceedance of the embedment stress in timber occurs here too, but only in the part of the nail between the two plastic hinges (**Error!**

Reference source not found.c). The second and the third mode represent ductile failure modes, due to the plastic hinges developed.

In the failure modes where plastic hinges arise, an elongation of the nail occurs, which generates an axial force in the nail, causing the so-called rope effect. This axial force compresses the timber girder and the RC slab against each other, and activates friction between the two materials. This phenomenon decreases the slip in the joint, thus increasing the total strength of the joint. In the Eurocode standard (EN 1995-1-1, 2004) it was adopted that contribution to the joint strength due to the rope effect can be taken as one fourth of the withdrawal capacity of the nail, but not greater than 15 % of the primary part of the capacity, denoted as Johansen's part. According to this, the final expressions for the analyzed joint strength are:

$$F_{v,Rk} = \min \begin{cases} f_{h,k} \cdot d \cdot t_{pen} \\ f_{h,k} \cdot d \cdot t_{pen} \left[\sqrt{2 + \dfrac{4 \cdot M_{y,Rk}}{f_{h,k} \cdot d \cdot {t_{pen}}^2}} - 1 \right] + \dfrac{F_{ax,Rk}}{4} \\ 2.3 \sqrt{M_{y,Rk} \cdot f_{h,k} \cdot d} + \dfrac{F_{ax,Rk}}{4} \end{cases} \quad (1)$$

where: $f_{h,k}$ – characteristic embedment strength of the timber,
d – nail diameter,
t_{pen} – penetration length,
$M_{y,Rk}$ – characteristic nail yield moment,
$F_{ax,Rk}$ – characteristic withdrawal capacity of the nail.

Characteristic embedment strength of the timber may be determined experimentally (EN 383, 2007), or using the formula for nails built-in into previously drilled holes:

$$f_{h,k} = 0.082 \cdot (1 - 0.01 \cdot d) \cdot \rho_k \quad (2)$$

where ρ_k is the characteristic value of the timber mass density in kg/m^3. Characteristic nail yield moment is determined based on the nail diameter and steel grade, according to the research (Blass, et al., 2001):

$$M_{y,Rk} = 0.3 \cdot f_u \cdot d^{2.6} \quad (3)$$

where f_u is the ultimate strength in MPa of the steel used for nail fabrication. Characteristic withdrawal capacity of the nail can be determined using the formula:

$$F_{ax,Rk} = f_{ax,k} \cdot d \cdot t_{pen} \quad (4)$$

where $f_{ax,k}$ is the characteristic withdrawal strength, determined by the formula:

$$f_{ax,k} = 20 \cdot 10^{-6} \cdot {\rho_k}^2 \quad (5)$$

According to the expressions (1), the strength of this type of joint is defined as a sum of the primary (Johansen's) strength and the secondary (rope effect) strength. The strength has to be calculated for every of the three failure modes, whereat the minimal value will be governing.

However, forming of the plastic hinges occurs at the beginning of the loading process, at small deformations in timber and in the nail. The rope effect arises much later, at much greater displacements in the joint, meaning that the failure mode of the joint depends only on the Johansen's strength, and in that phase the rope effect has no influence. Because of that, it is proposed to calculate the values of the Johansen's strength for every failure modes first, and than to determine the governing one. Finally, the rope effect strength should be included, if it exists for the governing failure mode.

For the calculation of the ultimate limit states and serviceability limit states of the composite structures, the stiffness of the joint is essential for determination of the static influences. According to the Eurocode, the stiffness is independent from the failure mode, and it is calculated by the formula:

$$K_{ser} = 2\rho_k^{1.5} d / 23 = 0.087\rho_k^{1.5} d \tag{6}$$

Using the formulas (1)-(6), the strength of a joint between a timber girder and an RC slab on trapezoidal steel sheeting is calculated for the analyzed case. For the adopted timber class C24, mass density was taken as ρ_k = 350 kg/m^3 (EN 338, 2009). Characteristic embedment strength of the timber, the nail yield moment, and the Johansen's joint strength are presented in Table 1.

Table 1 Characteristic values of the Johansen's part of strength for the analyzed joint

Item	Symbol	Unit	Value
Timber embedment strength	$f_{h,k}$	N/mm^2	26.7
Nail yield moment	$M_{y,Rk}$	Nmm	28350
Johansen's joint strength (mode 1)	$F_{v,Rk,1}$	N	18690
Johansen's joint strength (mode 2)	$F_{v,Rk,2}$	N	8140
Johansen's joint strength (mode 3)	$F_{v,Rk,3}$	N	5290

The lowest value of the Johansen's part of strength was obtained for the third failure mode (**Error! Reference source not found.**c), meaning that this is the governing mode. For this failure mode, the rope effect exists, so the secondary part of the joint strength was calculated (Table 2). At the end of the table, the calculated total strength and the slip modulus are presented.

Table 2 Characteristic values of the rope effect strength, total strength, and slip modulus of the analyzed joint

Item	Symbol	Unit	Value
Withdrawal strength	$f_{ax,k}$	N/mm^2	2.45
Nail withdrawal capacity	$F_{ax,Rk}$	N	1720
Rope effect strength 1 (0.25 $F_{ax.Rk}$)	$F_{re,Rk,1}$	N	430
Rope effect strength 2 (0.15 $F_{v,Rk,3}$)	$F_{re,Rk,2}$	N	790
Strength of the joint ($F_{v,Rk,3}$+ $F_{re,Rk,1)}$	$F_{v,Rk}$	N	5720
Slip modulus	K_{ser}	N/mm	3990

4. FE ANALYSIS OF THE JOINT AND COMPARISON OF RESULTS WITH THE ANALYTICAL EXPRESSIONS

Beside the analytical calculation, strength, stiffness, and failure mode of the analyzed joint have been determined, based on the numerical model, using FEM and software FEMAP with NX Nastran (NX Nastran User Guide, 2016). The model has been built applying line (1D) finite elements. The nail has been modelled using BEAM type elements. The size of the nail finite elements is 5 mm, and there are 20 elements (FE1-FE20), which have been set between successive nodes N1-N21 (Fig. 4).

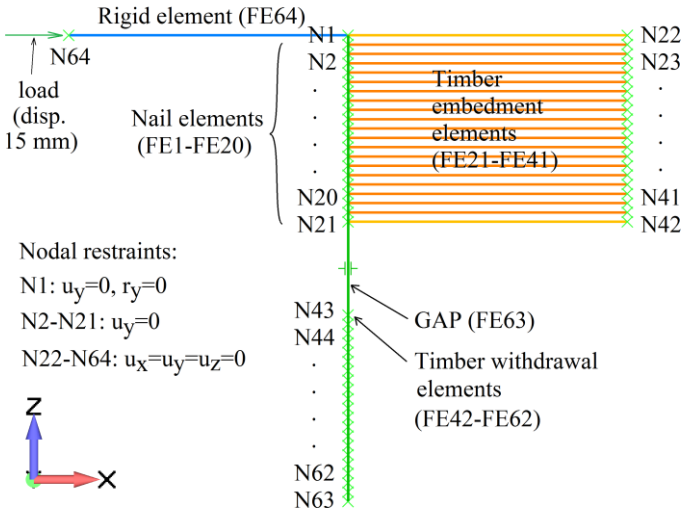

Fig. 4 Setting of the nodes and finite elements in the FEM model (N-node, FE-finite element, u-displacement, r-rotation)

Influence of the timber to the nail has been modelled with elements of ROD type. Behaviour of timber under embedment has been modelled with "timber embedment" elements (FE21-FE41), and behaviour of timber under withdrawal has been modelled with "timber withdrawal" elements (FE42-FE62). All elements lie in plane XZ. For "timber embedment" and "timber withdrawal" elements the length of 150 mm has been adopted. The cross-section area of these elements has been determined based on the embedment area of the nail FE, and it was 35 mm^2.

The material models for the steel of the nail have been adopted as elastoplastic (Fig. 5a). Material characteristics have been determined based on recommendations from literature (Hassanieh, et al., 2016; Nakashima, et al., 2013) and presented by a diagram (Fig. 5b).

Influence of the contact between the steel sheet and the timber has been modelled by GAP element (FE63). This element possesses high stiffness under compression and shear (C=10^9 N/mm), and does not possess tensile stiffness. The adopted friction coefficient was $\mu = 0.25$. This GAP element connects the nodes N1 and N63 (Fig. 4).

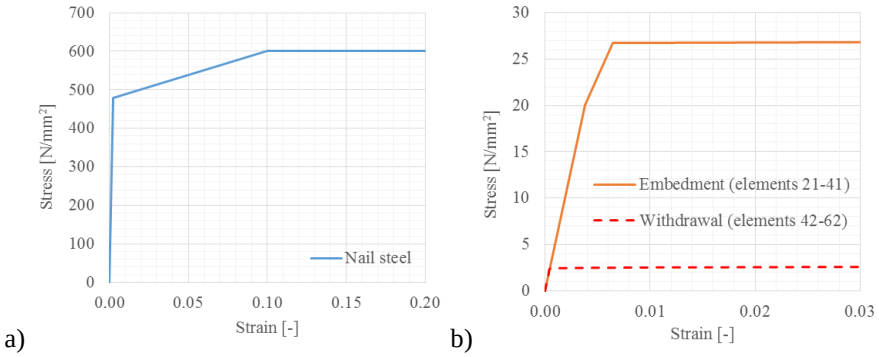

a) b)

Fig. 5 Stress-strain curves: a) nail steel, b) timber elements

The load is applied at the node N64, in the direction +X, as a displacement of 15 mm (EN 26891, 1991). This load acts on the nail via the ROD-type "rigid" element FE64. Introduction of the rigid element enables easy tracking of the force generated in the joint. Fig. 6 presents the load and the restrained nodes.

The proposed load acts in the X-direction, and the structure can deform only in XZ plane. Because of that, all nodes were restrained in Y-direction. Rotation of the cross-section of the nail at the slipping plane (node N1) is restrained around the Y-axis due to the stiffness of the RC slab, and the nodes N22-N64 are pinned supported.

An incremental nonlinear analysis with 200 steps has been conducted. Nonlinearity encompassed both the material and geometrical aspect of the structure. In this research, the joint strength has been analyzed in three ways:

1. Calculation of the total strength of the joint taking into account the primary (Johansen's) and secondary (rope effect) part of the strength;
2. Calculation of the total strength, as in variant 1, but with friction coefficient in the slipping plane taken as equal to zero;
3. Calculation of the total strength, as in variant 2, but with withdrawal strength of the nail taken as equal to zero.

According to the approaches described above, the following alterations have been made in the initial FE model. In the second variant (var. 2) the friction in the GAP element has been excluded ($\mu = 0$). The third variant of the model (var. 3) has been obtained by removing of the withdrawal elements (FE42-FE62) and the GAP element (FE63). Thus, the nail in the third variant does not possess withdrawal strength, and the rope effect is not present.

Fig. 6 present load-slip dependences for three different analyzed variants. The applied load corresponds to the axial force in the rigid element FE64, and the slip in the joint is equal to the displacement of the node N64 in X-direction. Within the same diagram, the contact force between the steel sheet and the timber, expressed as axial force in the GAP element, has been given for the first and the second variant of the joint, that is, for the variants in which the GAP element exists. The force in the GAP element is equal in both variant, as expected.

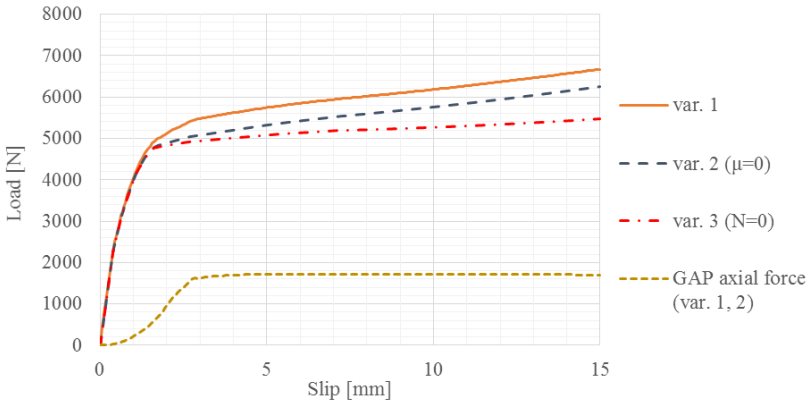

Fig. 6 Results. Load-slip curves for different variants of the joint and axial force in the GAP element for variants 1 and 2 (common curve)

In the Fig. 7 are given contour presentations of the bending moment for the variant 1 and variant 3. One may notice that plastic deformation occurred in the nail cross-sections with maximal bending moment. In this case two plasticized cross-sections occurred, one in the slipping plane, and the other in the timber volume at the depth approximately 30 mm below the slipping plane. The results shown in the Fig. 7 confirm that the failure modes obtained by Finite element analysis correspond to analytical calculation (Section 3, Table 1). Distribution and values of the bending moment in the variant 2 is identical with the variant 1, so they are not presented.

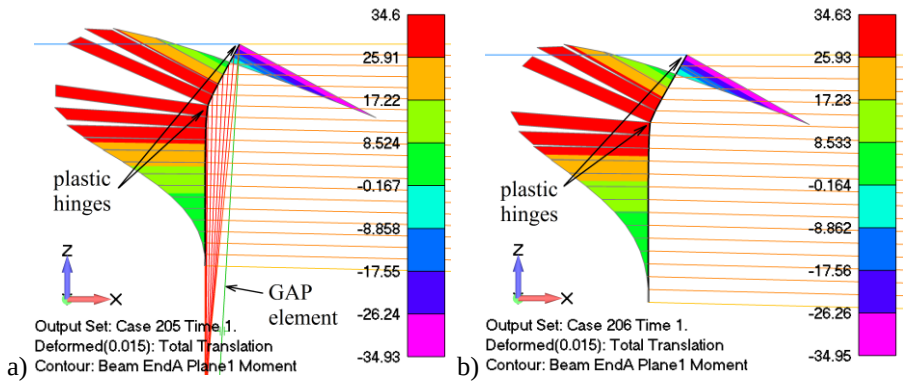

Fig. 7 Results. Deformed model and diagram of the bending moment in the nail: a) model variant 1, b) model variant 3

Table 3 presents comparative results of the numerical analysis and analytical calculation of the joint strength. In the FE analysis, the result value is the total strength of the joint, and one cannot obtain separate values for the primary (Johansen's) and secondary (rope effect) strength. Because of that, the Johansen's strength of the joint strength is identical with the total strength of the variant 3. The rope effect strength at variants 1 and 2 has been calculated as the

difference between the total strength and the Johansen's strength. Based on the load-slip dependence at 10 % and 40% of strength, the slip moduli have been calculated (EN 26891, 1991).

Table 3 Comparison of results between analytical expressions and numerical analysis

Item	Symbol	Unit	Analytical	var. 1	var. 2	var. 3
Primary (Johansen's) joint strength	$F_{v,Rk,3}$	N	5290	5480	5480	5480
Withdrawal force	$F_{ax,Rk}$	N	1720	1700	1700	-
Secondary (rope effect) strength	$F_{re,Rk,1}$	N	430	1190	770	-
Total joint strength	$F_{v,Rk}$	N	5720	6670	6250	5480
Slip modulus	K_{ser}	N/mm	3990	5230	5410	5940

From the diagram in Fig. 7 and from Table 3 one may notice that the rope effect exists even in the variant 2, although there is no friction between elements in the slipping plane. This is the consequence of the inclination of the part of the nail between the plastic hinges (Fig. 7). The axial force in the nail is then decomposed in two components, and the component in the direction of load acting increases the joint strength.

The difference of the Johansen's strength between the analytical and the numerical calculation are 3.5 %, confirming a very good agreement between the two methods. The rope effect strength show higher difference. For the variant 1, the FEM strength is 276% of the analytical one, and for the variant 2 the it is 179%.

5. CONCLUSION

The Eurocode standard does not define the procedure for calculation of the timber-concrete joint, so the procedure given for the timber-steel joints is used. In this paper three possible failure modes of the joint were analyzed. For the parameters considered, joint strength was the lowest in the third failure mode, where two plastic hinges occurred. Generally, steel exhibits ductile behaviour. Taking this into account, the failure modes of the analyzed joint that include occurrence of plastic hinges are considered favourable.

The Eurocode proposes one-stage joint calculation, using expressions that include the primary (Johansen's) strength and the secondary (rope effect) strength. According to this methodology, the governing failure mode is obtained as minimum of the summations of the primary and the secondary strength. The drawback of this procedure is that the rope effect is included into the determination of the governing failure mode. However, in reality, the governing failure mode is generated in early stage of the joint slipping, when rope effect has not been developed yet.

In this paper, a different methodology was proposed, that is, to calculate the primary strength first, for all failure modes. Based on these values, one should determine the governing failure mode, taking the minimal value. After that, the influence of the rope effect has to be added, in order to obtain the total strength of the joint.

In the paper, a complex numerical FEM model for the calculation of the considered joint has been developed. The model includes geometrical and material nonlinearity regarding the timber and the steel material. The status nonlinearity has been also included regarding the contact between the sheet metal and the timber at the slipping plane. This phenomenon has been treated applying the contact analysis with use of GAP finite element.

The results of the FE analysis and the proposed analytical calculation of the joint have been compared. The failure mode with two plastic hinges in the nail has been obtained applying both methods, thus showing good agreement.

The comparison of strength values between the analytical and the numerical method showed significant differences. The reason for this lies in the approach taken in the FEA. Namely, since the FEA gives total strength of the joint as a result, three separate analyses had to be concluded. Thereat, the nail element has been treated differently regarding the presence of possible effects:

- embedment strength, withdrawal strength, and friction;
- embedment strength and withdrawal strength;
- embedment strength only.

Based on this, the primary (Johansen's) strength and the secondary (rope effect strength) have been determined. The calculation according to the proposed analytical method and according to the numerical model produce results that are very close regarding the Johansen's strength only. Higher differences derive from the contribution of the rope effect strength, where the numerical model produces significantly higher strength values. These differences show a high reserve of the analytical method (both the existing and the proposed one) considering the calculation of the rope effect.

The proposed numerical method enables a more accurate analysis of this type of joint, with a remark that the embedment and the withdrawal behaviour of timber must be known.

Further improvement of this methodology would include implementing of test results of nail bending, timber embedment, and timber withdrawal behaviour into the FE model.

REFERENCES

1. H. J. Blass, A. Bienhaus, V. Krämer: Effective bending capacity of dowel-type fasteners, Proceedings PRO, pp. 71-80, 2001.
2. EN 1992-1-1: Eurocode 2: Design of concrete structures: Part 1-1: General rules and rules for buildings, 2004.
3. EN 1995-1-1: Eurocode 5: Design of timber structures: Part 1-1: General - Common rules and rules for buildings, 2004.
4. EN 26891:1991 - Timber structures. Joints made with mechanical fasteners. General principles for the determination of strength and deformation characteristics, 1991.
5. EN 338: Structural timber - Strength classes, 2009.
6. EN 383: Timber Structures - Test methods - Determination of embedment strength and foundation values for dowel type fasteners, 2007.
7. A. Hassanieh, H. R. Valipour, M. A. Bradford: Experimental and analytical behaviour of steel-timber composite connections, Construction and Building Materials, vol. 118, pp. 63-75, 2016.
8. A. Hassanieh, H. R. Valipour, M. A. Bradford: Load-slip behaviour of steel-cross laminated timber (CLT) composite connections, Journal of Constructional Steel Research, vol. 122, pp. 110-121, 2016.
9. K. W. Johansen: Theory of Timber Connections, Int Assoc Bridge Struct Eng, vol. 9, pp. 249-262, 1949.
10. N. Khorsandnia, H. R. Valipour, C. Keith: Experimental and analytical investigation of short-term behaviour of LVL-concrete composite connections and beams, Construction and Building Materials, vol. 37, pp. 229-238, 2012.
11. Lj. Kozarić: Vibracije izazvane ljudskim delovanjem kod spregnutih međuspratnih konstrukcija tipa drvo-laki beton, doktorska disertacija, Subotica, Građevinski fakultet, 2016.
12. E. Maslak, D. Stojić, D. Drenić, E. Mešić, R. Cvetković: Strengthening timber-concrete composite girders with prestressed reinforcement, Građevinar, vol. 72, pp. 1001-1010, 2020.
13. M. Milić, P. Petronijević, T. Vacev, I. Nešović, A. Zorić: Rehabilitation of a Wooden Floor Structure by Composite Joint with RC Slab, Contemporary Achievement in Civil Enginnering, Subotica, Građevinski fakultet, pp. 203-209, 2021.

14. S. Nakashima, A. Kitamori, T. Mori, K. Komatsu: Propose Alternative Design Criteria for Dowel Type Joint with CLT, RILEM International Symposium on Materials and Joints in Timber Structures, Stuttgart, Germany, 739-748, 2013.
15. B. Stevanović: Eksperimentalna i teorijska analiza spregnutih nosača drvo-beton izvedenih mehaničkim spojnim sredstvima, Materijali i konstrukcije, pp. 29-46, 2004.
16. D. Stojić, R. Cvetković: Analysis of a composite timber-concrete structures according to the limit states: Design and innovative methods in coupling of a timber and concrete, Facta universitatis - series: Architecture and Civil Engineering, pp. 169-184, 2001.

PRORAČUN VEZE DRVO-BETON IZVEDENE EKSEROM PREMA EVROKODU I PRIMENOM MKE

Prilikom sanacije stambenih objekata građenih u toku prve polovine prošlog veka, potrebno je ojačati drvene međuspratne konstrukcije kako bi ispunile zahteve nosivosti i upotrebljivosti prema savremenim propisima. Međuspratne konstrukcije od monolitnih drvenih nosača se najjednostavnije ojačavaju sprezanjem sa armirano-betonskom pločom koja se izrađuje na trapeznom čeličnom limu, a spajanje se vrši odgovarajućim spojnim sredstvima. U radu je prikazan postupak proračuna eksera koji se koristi kao moždanik za sprezanje drveta i betona. Postupak je zasnovan na jednačinama datim u Evrokodu 5, a pored toga je sproveden i proračun primenom MKE i dato je poređenje rezultata.

Ključne reči: *sprezanje drvo-beton, ekser, efekat užeta, Evrokod 5, MKE*